SCIENTIFIC REPORTS

OPEN

SUBJECT AREAS:
SOLID EARTH SCIENCES
GEOMORPHOLOGY

Received
9 September 2013

Accepted
24 February 2014

Published
11 March 2014

Correspondence and requests for materials should be addressed to J.J.Q. (qujianj@lzb.ac.cn)

The sand-deposition impact of artificial gravel beds on the protection of the Mogao Grottoes

Guo Shuai Li[1,2,3,4], Jian Jun Qu[4,5], Xu Zhi Li[2] & Wan Fu Wang[6]

[1]Institute of Remote Sensing and Digital Earth, Chinese Academy of Sciences, Beijing 100094, China, [2]Technology and Engineering Center for Space Utilization, Chinese Academy of Sciences, Beijing 100094, China, [3]University of Chinese Academy of Sciences, Beijing 100049, China, [4]Dunhuang *Gobi* and Desert Ecological and Environmental Research Station, Cold and Arid Regions Environmental and Engineering Research Institute, Chinese Academy of Sciences, Dunhuang 736200, China, [5]Cold and Arid Regions Environmental and Engineering Research Institute, Chinese Academy of Sciences, Lanzhou 730000, China, [6]Dunhuang Academy China, Dunhuang 736200, China.

Gravel beds can prevent sand-dust emission and weaken sand-dust flux. We used wind-tunnel experiments and field observations on artificial gravel beds above the Mogao Grottoes to quantify their impact. In the report, we identified a significant correlation between gravel roughness and its ability to trap wind-transported sand. The optimal combinations of gravel diameter and coverage were determined. The greatest roughness is achieved when small gravel coverage is 75%, medium 40% and large 45%. We found that initial wind speed and gravel coverage are the key factors controlling the amount of sand trapped by the gravel beds.

The protective measures employed for controlling sand disasters have focused principally on mechanical, vegetation and chemical defense[1]. The Mogao Grottoes (40°5′17.25″N, 94°40′16.67″E) is a famous world cultural heritage site located on the desert margins in western Gansu Province, China. They contain 45,000 m^2 of priceless Buddhist murals, 2,500 painted sculptures, and 492 caves[2]. However, destructive aeolian sand has threatened the murals in the Mogao Grottoes since the Five Dynasties (907–960 C.E.). The grotto murals have been consistently weathered over the centuries by aeolian sand through wind erosion, wind accumulation and dust suppression. Many protective measures have been adopted (Fig. 1), but they have not achieved their stated aims[3]. Prevailing local harmful winds are principally northwesterlies, with westerlies and southwesterlies of secondary importance. When they blow across the land surface, sand accumulation occurs. As a general rule, aeolian sand does not blow easily across wind-eroded *gobi* surfaces, especially on the borders between gravel beds and desert lands. Here, wind-eroded *gobi* refers to a land surface covered by only a thin layer of large diameter gravel, the lower layers being an admixture of sandy gravel and earthy deposits. For hindering the transference of sand from nearby Mount Mingsha to the grottoes,creating artificial gravel beds is an effective way to reduce aeolian sand damage of the Mogao Grottoes. We developed artificial gravel beds above the Mogao Grottoes with varied gravel diameters and coverage based upon the original topography (cobbles, sand gravel beds, and sandy gravel beds). Increased surface roughness and resulted in changes to air flow made these artificial gravel beds effective for controlling secondary dust flux and weakening the sediment transport intensity of sand-carrying wind.

The earliest studies of gravel beds were by Redway[4] and Osborn[5]. *Gobi* dust storms are common in arid environments[6]. At the macro-scale, Jugder *et al.*[7] studied the spatial and temporal distribution of dust mass concerntrations of PM10 and PM2.5 in the *Gobi* Desert in Mongolia, whilst Zhou and Huang[8] studied the momentum and sensible heat fluxes of turbulent transfer characteristics on a *gobi* surface in Dunhuang, China. These macro-scale studies revealed the characteristics of sand drifts and air flow fields, but studies of the concrete interaction between sand and *gobi* are increasingly the focus of attention. Nickling and Neuman[9] investigated the deflation drags associated with various diameters and spacings of glass spheres substituted for gravel in wind-tunnel tests. The relations between the drag coefficients of *gobi* surfaces, gravel diameter and coverage were defined by Dong *et al.*[10]. Subsequently, Mikami *et al.*[11] used a sand particle counter (SPC) with a laser beam transmitter and receiver to research saltation fluxes at different heights above *gobi* surfaces combined with meteorological elements. Zhang *et al.*[12] convincingly interpreted the structure of wind-blown sand on *gobi*

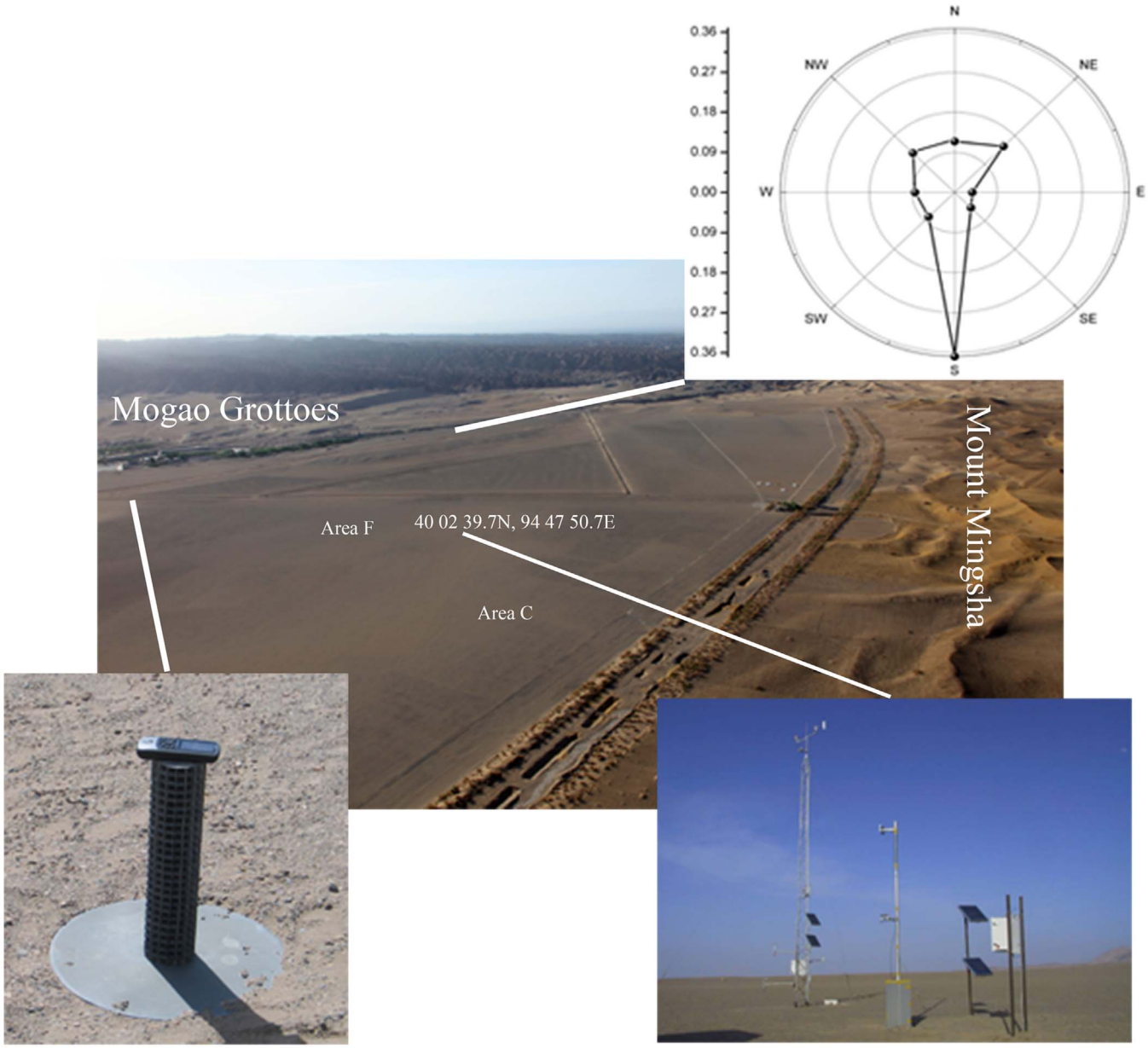

Figure 1 | **Study site above the Mogao Grottoes.** In the gravel bed above the Mogao Grottoes were a sand-accumulation instrument with 16 orientations (lower left) and a Japanese HOBO weather station (lower right). Upper right is a wind rose derived from wind measurements above the Mogao Grottoes during 1992–2008. Area C had a treated surface (large gravel, 30% coverage) and a non-treated surface (medium gravel, 30% coverage); Area F had a treated surface (medium gravel, 30% coverage) and a non-treated surface (medium gravel, 30% coverage). The white lines point to the measuring sites. The photographs were provided by G. S. Li and W. F. Wang.

surfaces and found that blown-sand activities on such surfaces are mainly concentrated at heights below 20 cm. Gao *et al.*[13] studied the aerodynamic roughness and drag coefficients of *gobi*, whereas Wu[1] found that gravel beds could increase aerodynamic roughness and inhibit wind erosion.

Generally, the variation of sand weights at different heights decreased exponentially[14,15], but Qu *et al.*[16] proposed that the distribution of sand particle weights at different heights on *gobi* surfaces does not simply follow logarithmic or exponential laws. Instead, with extreme sand weight the *gobi* surface height will increase as the wind speed increases. Dong *et al.*[17] thought that maximal aerodynamic roughness length occurs at gravel coverage ranges between 40%–70%. On that basis, Liu *et al.*[18] made a detailed study of the relation between gravel coverage and diameter, and concluded that the combination of 30% of gravel coverage and gravel of a 2–4 cm diameter could resist 50% of the sand drift weight. Tan *et al.*[19] proposed that the change in the sand transport rates of *gobi* surfaces in relation to height follows a quadratic polynomial. Liu *et al.*[18] and Tan *et al.*[19], in a wind-tunnel experiment involving various gravel diameters, gravel coverage and sand weights, also demonstrated that by building an artificial *gobi* surface with a gravel coverage of 30%, a dynamic wind-blown sand flux equilibrium could be achieved. Zhang *et al.*[20] studied the vertical distribution of wind-blown sand flux and attempted to quantify sand erosion and deposition above gravel beds.

At present, few analyses of the effect of optimum gravel diameter, gravel roughness and other relative influencing factors on artificial sand beds are available. In this study, we have systematically analyzed the characteristics of gravel bed sand deposition using field wind-tunnel experiments and field observations. In field wind-tunnel experiments, the relations between wind speed, abrasion time, sand

flux structure, gravel coverage and roughness were quantitatively analyzed; and the real impact of sand deposition on gravel beds was investigated in the field with sand-accumulation instruments and sand-accumulation buckets.

Results

Characteristics of the original gravel bed. There is a Japanese HOBO weather station located on the gravel bed (Fig. 1) but it is a considerable distance from the shifting sands on Mount Mingsha, and wind speed and wind direction data (sampling frequency: 10 min) for 2005–2008 from that station indicate that wind speed weakens by the time it reaches the weather station. The Supplementary Text states that the static pressure threshold wind speed of 10.6 m/s at a height of 2 m on the shifting sand surface on Mount Mingsha are taken as the threshold wind speed above the Mogao Grottoes (see Supplementary Fig. S1 online).

Gravel paving was laid above the grottoes in 2009–2010; even if this does not directly affect the threshold wind speed in the shifting sand area, the dynamics of this process and the paved area might have influenced our analysis, so data from that period was not considered in this study. Vis-à-vis the wind direction datasets recorded at the HOBO weather station for the purposes of observing gravel bed interiors, "sand-blowing wind" is defined as wind with sand particles which blows from the N, NNE, NE, ENE, E, ESE, SE, SSE or S; "sand-carrying wind," which in fact contains sand particles from sand-blowing wind, is defined as the primary harmful wind blowing from Mount Mingsha to the grottoes from a SSW, SW, WSW, W, WNW, NW or NNW direction. More specifically, sand-blowing wind does not carry sand particles when first blowing over the gravel bed, but rather collects sand particles as it blows. Maximum wind speeds and wind directions for 2005–2008 are shown in Supplementary Fig. S1 online. Table 1 shows that sand-blowing winds and sand-carrying winds most often occur during the summer and spring on the original gravel bed above the Mogao Grottoes.

Aeolian sand data collected by sand-accumulation instruments with 16 orientations for 2004–2006 (Fig. 1) provide information on sand transport characteristics for the original gravel bed above the Mogao Grottoes. Supplementary Fig. S2 online presents transported sand weight as a percentage of the total from different orientations as found on the original gravel bed near the grottoes' sides. It shows that transported sand weight from a NNE direction was 20.37% of the total transported sand weight; E, 15.21%; ENE, 10.73%; NE, 9.63%; ESE, 8.98%; N, 8.14%; SE, 1.97%; S, 1.27%; and SSE, 0.93%. The percentages of transported sand weight from a NNW direction were 8.21%; WNW, 5.82%; NW, 2.51%; SW, 1.98%; W, 1.69%; WSW, 1.35%; and SSW 1.20%. Thus, dust storms occurring on the original gravel bed are caused principally by sand-blowing winds, while the main function of the artificial bed is to prevent further sand transport by sand-blowing winds.

Characteristics of artificial gravel beds. *Gravel coverage, wind speed and abrasion time.* Wind speed and abrasion time determined the sand weight deposited on the gravel, and thus ultimately determined the coverage of the gravel still exposed above the sand's surface.

Table 1 | The frequency and abrasion time for both sand-blowing wind and sand-carrying wind (the sand-blowing wind containing sand) on the original gravel bed in 2005–2008

	Sand-blowing wind		Sand-carrying wind	
	Frequency	Abrasion time (h)	Frequency	Abrasion time (h)
Spring	43 events	28.5	30 events	13
Summer	54 events	28	51 events	12.7
Autumn	6 events	26.7	9 events	2.3

Gravel coverage was also influenced by the roughness of the gravel. Also, the sand weight at different heights influenced the coverage of the gravel exposed above the sand's surface.

The relations between wind speed, abrasion time, and coverage of small, medium, and large gravels were obtained from 2004 field wind-tunnel experimental data. In that experiment, wind speeds were quantitatively controlled at about 8 m/s, 10 m/s, 12 m/s, 14 m/s, 16 m/s and 18 m/s. We used ARC INFO 8.3 software (ESRI Corp., Redlands, California) for the vectorization of some sample blocks of gravel bed wind-blown for differing times; the percentage of total surface area that had gravel >2 mm was then entered into the statistical computing functional module, and the coverage calculated. The respective relations between wind speed U_s (m/s) and coverage Cov_s (%), and abrasion time T_s (min) and coverage Cov_s (%) of small gravel can be expressed as:

$$Cov_s = 28.169 - 0.919 \times U_s + 0.915 \times U_s^2,\ R^2 = 0.99 \quad (1)$$

$$Cov_s = 29.770 + 176.838/T_s,\ R^2 = 0.98 \quad (2)$$

The respective relations between wind speed U_m (m/s) and coverage Cov_m (%), and abrasion time T_m (min) and coverage Cov_m (%) of medium gravel can be expressed as:

$$Cov_m = -18.755 + 27.644 \ln U_m,\ R^2 = 0.98 \quad (3)$$

$$Cov_m = 73.840 - 3.400T_m + 0.129T_m^2 - 0.001T_m^3,\ R^2 = 1.00 \quad (4)$$

The respective relations between wind speed U_L (m/s) and coverage Cov_L (%), and abrasion time T_L (min) and coverage Cov_L (%) of large gravel can be expressed as:

$$Cov_L = 21.749 + 1.447U_L + 0.093U_L^2,\ R^2 = 0.95 \quad (5)$$

$$Cov_L = 98.904 - 6.218T_L + 0.214T_L^2 - 0.003T_L^3,\ R^2 = 0.94 \quad (6)$$

Thus, the relation between wind speed and coverage of small and large gravel fits the quadratic function; the relation between abrasion time and coverage of medium and large gravel fits the cubic function; the relation between abrasion time and coverage of small gravel fits the reciprocal function; and the relation between wind speed and coverage of medium gravel fits the logarithmic function. The mathematical formats of these factors provide an insight into their interactions.

Sand weight, wind speed and height. Analysis of field wind-tunnel experimental data in 2011 showed that a 20% coverage of small gravel approximated to a 23.53% coverage in the original gravel bed. To reduce costs, a coverage of 30% of medium and large gravels for the artificial gravel bed was shown to be both practical and appropriate. As for the underlying sedimentary layer, a coverage of 15%–20% of small gravel proved to be adequate. Thus, 20% small gravel and 30% medium and large gravels approximated the characteristics of the original gravel bed and the artificial gravel bed above the Mogao Grottoes, respectively.

The relation between wind speed U_p (m/s) and the correlative sand weight Q_p (g) at varying heights (1 cm, 3 cm, 5 cm, 9 cm, 13 cm and 17 cm) under controlled initial wind speeds (8 m/s, 10 m/s, 12 m/s and 14 m/s) in the original gravel bed (small gravel, 20% coverage) are expressed according to the maximum value of R^2 using these standard formulae:

$$Q_{p8} = 3.346 + 12.725U_{p8} - 3.045U_{p8}^2 + 0.180U_{p8}^3,\ R^2 = 0.96 \quad (7)$$

$$Q_{p10} = -26.338 + 22.196U_{p10} - 3.448U_{p10}^2 + 0.154U_{p10}^3,\ R^2 = 0.99 \quad (8)$$

$$Q_{p12} = -1.977 + 2.719U_{p12} - 0.186U_{p12}^2,\ R^2 = 0.81 \quad (9)$$

$$Q_{p14} = -1.569 + 1.680U_{p14} - 0.098U_{p14}^2,\ R^2 = 0.84 \quad (10)$$

where the subscripts $p8$ through $p14$ refer to the initial wind speeds described above. These same relations pertaining to a mixture of medium and large gravel of 30% coverage are expressed as:

$$Q_{a8} = 6.488 + 1.719U_{a8} - 0.460U_{a8}^2 + 0.022U_{a8}^3,\ R^2 = 0.97 \quad (11)$$

$$Q_{a10} = 3.972 + 6.083U_{a10} - 0.835U_{a10}^2 + 0.026U_{a10}^3,\ R^2 = 0.88 \quad (12)$$

$$Q_{a12} = -18.163 + 11.607U_{a12} - 1.322U_{a12}^2 + 0.043U_{a12}^3,\ R^2 = 0.87 \quad (13)$$

$$Q_{a14} = -47.777 + 19.072U_{a14} - 1.930U_{a14}^2 + 0.060U_{a14}^3,\ R^2 = 0.67 \quad (14)$$

Thus, initial wind speed (wind speed calculated as net wind when blowing into the gravel bed area) and gravel coverage are key factors that affect accumulated sand weights in the gravel bed. However, the effect of sand weight as related to gravel diameter is not quite as clear-cut. The relation between wind speed and accumulated sand weight at the same height fits the cubic function at lower initial wind speeds in the original gravel bed; this changes into the quadratic function with an increase in initial wind speed. However, in the artificial gravel bed, regardless of how great the initial wind speed is, the relation between wind speed and accumulated sand weight at the same height always fits the cubic function, but the correlation becomes smaller with an increase in initial wind speed. Understanding more about these relations could help us to apply them better in practice.

According to our analysis of 2011 field wind-tunnel measurement data, sand weight (%) in the original gravel bed (small gravel, 20% coverage) presented a certain regularity along a vertical direction under the influence of different initial wind speeds. At a height of 0–6 cm from the surface, the size distribution of sand weight (%) were Q (8 m/s) > Q (10 m/s) > Q (12 m/s) > Q (14 m/s); at a height of 10–20 cm from the surface, the size distribution of sand weight (%) were Q (14 m/s) > Q (12 m/s) > Q (10 m/s) > Q (8 m/s). Accumulated sand weight at a height of 0–2 cm was maximal (20.95%) when initial wind speed was 8 m/s; sand weight at a height of 2–4 cm was maximal (16.82%) at 10 m/s; sand weight at a height of 4–6 cm was maximal (14.82%) at 12 m/s; and sand weight at a height of 4–6 cm was maximal (14.22%) at 14 m/s (Fig. 2). Thus, the sand weight maximum decreased with an increase in initial wind speed.

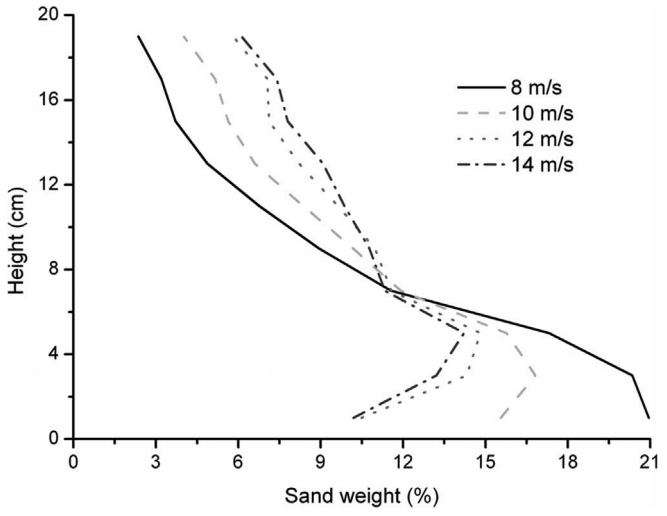

Figure 2 | Distribution of sand weights at various heights in the original gravel bed under different initial wind speeds. Small gravel (20%) bed is very close to the coverage 23.53% of the original gravel bed.

Sand weight outlines in medium gravel (30% and 40%) were more regular than in large gravel (30% and 40%). Vis-à-vis the size distribution of sand weight in medium gravel (30%) at a height of 8–20 cm, it was Q (14 m/s) > Q (12 m/s) > Q (10 m/s) > Q (8 m/s) (Fig. 3a1); in large gravel (30%) at heights of 8–20 cm and 14–20 cm it was Q (14 m/s) > Q (12 m/s) > Q (10 m/s) > Q (8 m/s) (Fig. 3b1); in medium gravel (40%) at a height of 6–10 cm it was Q (8 m/s) > Q (10 m/s) > Q (12 m/s) > Q (14 m/s) (Fig. 3a2); and in large gravel (40%) at a height of 18–20 cm it was Q (14 m/s) > Q (12 m/s) > Q (10 m/s) > Q (8 m/s) (Fig. 3b2). Thus, the distribution of accumulated sand weights at increasing heights became irregular with increases in gravel diameter and coverage.

This demonstrates that accumulated sand weight in the original gravel bed follows a definite law along a vertical direction in response to different initial wind speeds. Sand weight decreased with an increase in initial wind speeds at a height of 0–8 cm, and increased with an increase in initial wind speeds at a height of 10–20 cm. The distribution of accumulated sand weights in medium gravel at various heights was more regular than that in large gravel on the artificial gravel bed.

Roughness and gravel coverage. Our analysis of 2011 field wind-tunnel experimental data indicated that roughness associated with different gravel coverage can be revealed by an equilibrium wind speed profiler when the height of the wind speed profiler and the net wind speed are combined with Supplementary Text Eq. (16). The roughness curves of small, medium and large gravels presented four peaks related to the increase in coverage (Fig. 4). Fig. 4 suggests that the following combinations of diameter and coverage are appropriate for gravel paving on the gravel bed above the grottoes: small gravel, 75%; medium gravel, 40%; and large gravel, 45%. To reduce the labor costs of gravel paving the area, the small gravel could be the underlayment, with an emphasis for overlay on the medium and large gravels. The protective effect of gravel paving can thus be maximized by following this construction sequence: first, small gravel (1–2 cm) is spread to a ground coverage up to 15%–20% on a treated earth surface, and then larger gravel (3–5 cm) is randomly spread to a ground coverage up to 30%–40%.

Comparison of original and artificial gravel beds. *Field wind-tunnel experiments*. The sand accumulation rate is expressed as sand weight deposited from sand-carrying wind per unit width against unit time. In our study, the size distribution of sand accumulation rates on the original gravel bed (small gravel, 20% coverage) at a height of 0–14 cm was Q_d (14 m/s) > Q_d (12 m/s) > Q_d (10 m/s) > Q_d (8 m/s) > Q_d (6 m/s) (Fig. 5). The sand accumulation rate thus increased with an increase in initial wind speed: the higher the initial wind speed blowing into the original gravel bed area, the greater the rate of sand accumulation.

The impact of sand accumulation in medium (30% coverage) (Fig. 6a1) and large gravel (30%) (Fig. 6b1) areas in the artificial gravel bed was greater than in the original gravel bed (small gravel, 20%) (Fig. 5). The size distribution of sand accumulation rates in the medium gravel bed with 30% coverage at a height of 0–14 cm was Q_d (14 m/s) > Q_d (12 m/s) > Q_d (10 m/s) > Q_d (8 m/s) > Q_d (6 m/s). Sand accumulation rates at height 0–2 cm were maximal at initial wind speeds of 6 m/s, 8 m/s, 10 m/s and 12 m/s, but the sand accumulation rate at height 6–8 cm was maximal with an initial wind speed of 14 m/s (4.65 g/(min·m)) (Fig. 6a1). The sand accumulation rate over large gravel (30% coverage) at height 0–2 cm was up to 7.34 g/(min·m) with an initial wind speed of 12 m/s (Fig. 6b1). The size distribution of the sand accumulation rate of medium gravel (40% coverage) at height 0–12 cm was Q_d (14 m/s) > Q_d (12 m/s) > Q_d (10 m/s) > Q_d (8 m/s) > Q_d (6 m/s) (Fig. 6a2). The size distribution of sand accumulation rates for large gravel (40% coverage) were more irregular (Fig. 6b2).

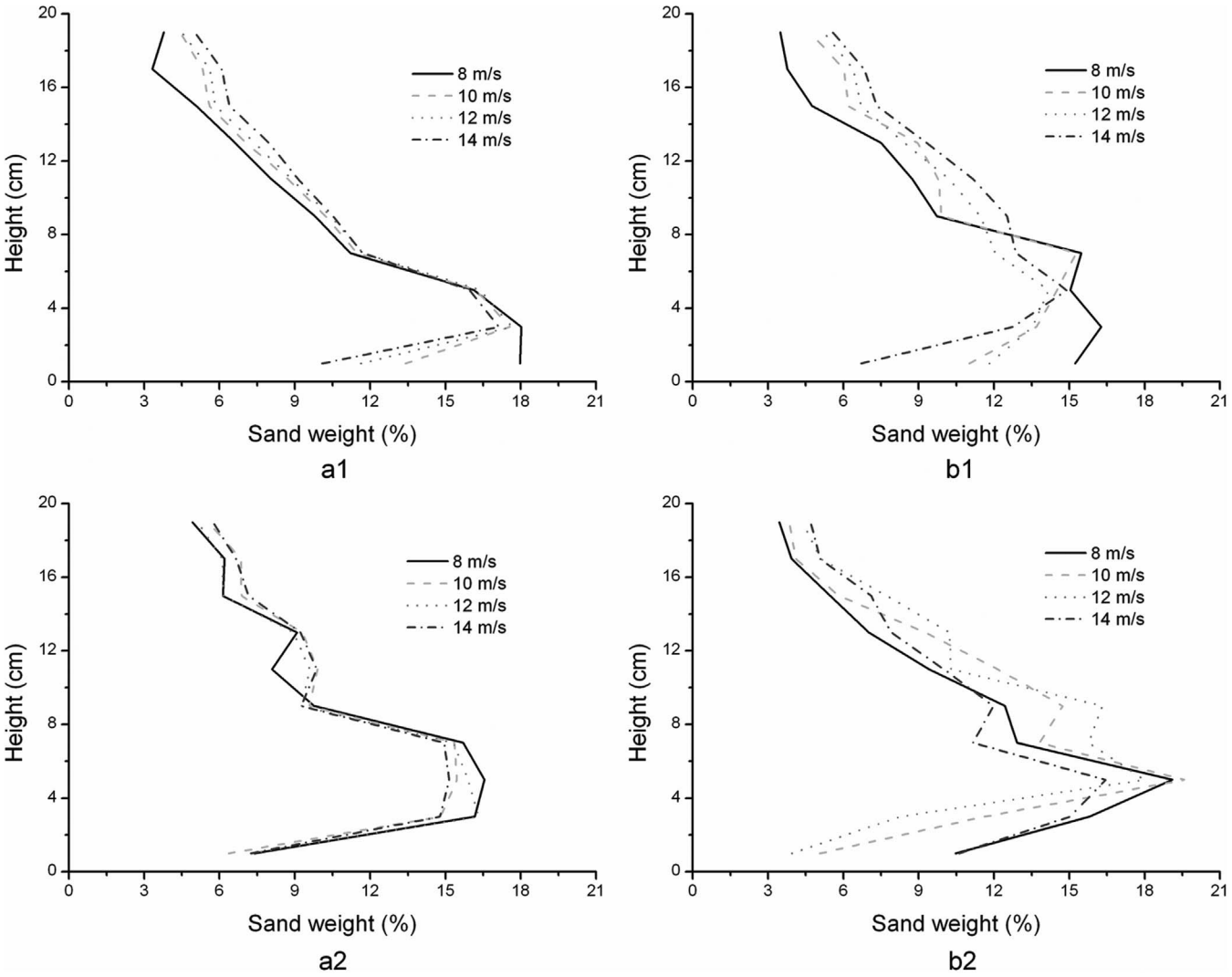

Figure 3 | Distribution of sand weights at various heights in the artificial gravel bed under different initial wind speeds. (a1) Variations in accumulated sand weights at various heights on a medium gravel (2–4 cm) bed with coverage of 30% under different initial wind speeds (8 m/s, 10 m/s, 12 m/s, and 14 m/s). (a2) On a medium gravel (2–4 cm) bed with coverage of 40%. (b1) On a large gravel (4–6 cm) bed with coverage of 30%. (b2) On a large gravel (4–6 cm) bed with coverage of 40%.

On the artificial gravel bed, the sand accumulation rate for small gravel and its consequent impact became greater with increased coverage. Conversely, the sand accumulation rate for large gravel became smaller with increased coverage and its overall impact became negligible. Therefore, on the whole, the impact of sand accumulation for a combination of small (40% coverage) and large gravel (30%) proved optimal. In addition to the gravel paving's main function of preventing sand-driven by wind, intercepting sand particles from sand-carrying wind also serves a vital purpose.

Field observation experiments. We analyzed a sand accumulation section (W → E) on the northern side of a V-shaped nylon net[3] in Areas C (treated surface: large gravel, 30%; non-treated surface: medium gravel, 30%) and F (treated surface: medium gravel, 30%; non-treated surface: medium gravel, 30%) of an experimental area of gravel paving (Fig. 1). Data are for the periods March 18 – April 15, 2009 (Phase 1) and May 13 – May 17, 2010 (Phase 2). The purpose was to study the effect of sand accumulation on original and artificial gravel beds (large gravel 30%, medium gravel 30%).

In Phase 1, the easterly wind had an initial wind speed of more than 10.6 m/s at a height of 2 m (average wind speed was 11.67 m/s, and abrasion time 30 min); this was defined as the net wind speed (sand-blowing wind). In Phase 2 the westerly wind had a wind speed of more than 10.6 m/s at a height of 2 m (average wind speed was 11.77 m/s, abrasion time 15 min), so this was defined as the sand-carrying wind. In Phase 1, the average sand accumulation rate over the original gravel bed was 0.042 g/(min·m) when a sand-blowing wind was present; in Phase 2, the average was −0.171 g/(min·m) after the sand-carrying wind had passed. In Phase 1, average sand accumulation rates for large (30%, treated surface) and medium gravel (30%, treated surface) were −0.219 g/(min·m) and 6.075 g/(min·m), respectively, when a sand-blowing wind was present; In Phase 2, these averages were 0.292 g/(min·m) and 1.938 g/(min·m), respectively, after the sand-carrying wind had passed.

Contrary to expectations, over the original gravel bed the sand accumulation rate was positive when a sand-blowing wind was present, and negative after a sand-carrying wind had passed. These abnormalities in sand accumulation rates in the original gravel bed are an important cause of severe aeolian sand damage in the Mogao Grottoes. The sand accumulation rate of large gravel (30% coverage, treated surface) in the paved gravel experimental area was negative when a sand-blowing wind was present and positive after a sand-carrying wind had passed; this shows that large gravel (30%, treated

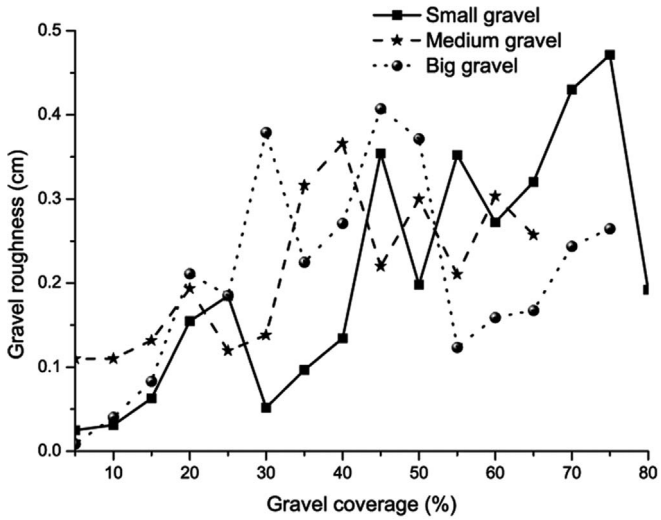

Figure 4 | Variations in the roughness of small, medium, and large gravel against increases in coverage. Coverage of relatively small gravel (and aerodynamic roughness lengths) are 25% (0.185 cm), 45% (0.354 cm), 55% (0.352 cm) and 75% (0.471 cm); those of medium gravel are 20% (0.193 cm), 40% (0.366 cm), 50% (0.300 cm) and 60% (0.303 cm); and those of large gravel are 20% (0.211 cm), 30% (0.379 cm), 45% (0.407 cm) and 75% (0.265 cm).

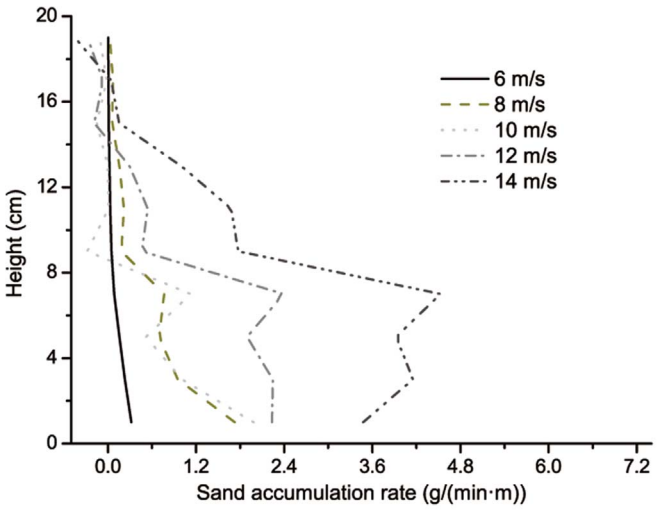

Figure 5 | Distribution of sand-accumulation rates at various heights on the original gravel bed under different initial wind speeds. Sand-accumulation rates (g/(min·m)) of a small gravel (20%) bed under different initial wind speeds (6 m/s, 8 m/s, 10 m/s, 12 m/s and 14 m/s).

surface) corrected the abnormal sand accumulation rate in the original gravel bed. The sand accumulation rate of medium gravel (30%, treated surface) in the paved gravel experimental area was positive when a sand-blowing wind was present, similar to that of the original gravel bed, but the sand accumulation rate was also positive at 1.938 g/(min·m) after a sand-carrying wind had passed; this rate was significantly greater than the sand accumulation rate of 0.292 g/(min·m) for large gravel (30%, treated surface). This suggests that the impact of sand accumulation on medium gravel (30%, treated surface) is more effective vis-à-vis protection against sand than on large gravel (30%, treated surface) when a sand-carrying wind passes. Therefore, the data suggest that gravel paving using a combination of large gravel (30%) and medium gravel (30%) is both appropriate and effective.

On June 2, 2011 a great dust storm (NW wind) occurred in the vicinity of the grottoes, and measurement data were acquired from sand-accumulation instruments stationed at a height of 1 m along a NW → SE orientation above the grottoes. The weight of accumulated sand in the paved gravel area was approximately 21% less than in the shifting sand area at height 0–18 cm (Fig. 7). This indicates that the gravel paving captured 21% of the sand from the sand-carrying wind, with effective sand accumulation rates. This gravel paving model thus shows significant applicability.

Discussion

The gravel paving of the original gravel bed above the Mogao Grottoes addresses many research questions relating to gravel armoring to reduce wind erosion. Its protective mechanism has scientific validity and plays an important role in aeolian sand protection for infrastructure such as railways, spaceflight, satellite and military bases in aeolian sand and *gobi* areas.

In the relation between gravel coverage and gravel roughness, we determined optimal coverage by gravel with different diameters using the peak values of gravel roughness. This fundamentally agreed with the perspective of Dong *et al.*[17] that aerodynamic roughness length possesses maximal value when gravel coverage is in the range of 40%–70%. However, we further refined the specific optimal gravel coverage, diameter and roughness, as shown in Fig. 4. The peaks in Fig. 4 indicate that small gravel has the greatest roughness at ~75% coverage; medium gravel has the greatest roughness at ~40% coverage; and large gravel has the greatest roughness at ~45% coverage. We proposed that sand particles in the gravel bed would be blown by a sand-blowing wind and deposited by a sand-carrying wind. This differentiation between the blowing of unsaturated sand drift and the accumulation of saturated sand drift in the gravel bed is in accordance with the findings of Zhang *et al.*[20]. It also showed that the sand accumulation rate could be regarded as an index for efficiently measuring erosion and deposition in the gravel bed.

However, the secondary flow and size effect problems caused by the wind tunnel wall in our study remained unresolved. In observations of aeolian sand transport, a field wind tunnel could ideally be used to simulate the pulsation of wind speed and wind direction resulting from thermal convection caused by actual ground surface temperature changes. Such a tunnel could also be used to model dust-rolling phenomena. Neither of these were possible with the wind tunnel that was available to us. In future, we intend to use a combination of a particle image velocimetry (PIV) system and a field wind tunnel in the gravel bed to determine how gravel characteristics influence the incidence of sand particles and the distribution of fluctuating speeds. Problems were also posed by density and 3-D velocity distributions for sand saltation rates vis-à-vis different gravel diameters, coverage, and shapes at different heights in the gravel bed.

Other drawbacks in our study included the automatic weather station not being set up on the surface of shifting sand to monitor change when measuring static pressure threshold wind speed for shifting sand surfaces. There were pulses in the wind speed from the field wind-tunnel fan, indicating that it was not controlled accurately; errors were in the range of 0.3 m/s. Our calculation of the weight of sand carried by the sand-carrying wind as reduced by gravel paving was based on only one dust storm where it should have been calculated from the average of many dust storms. Further, human and natural factors were not accurately controlled, and thus possibly disturbed the data.

Methods

Gravel bed processing. After proposing the artificial gravel bed concept we performed some experiments. Our experimental method was quite complicated, involving three gravel diameters and different coverage (15%, 30%, 30%–40%, 45%, and 50%–60%). First, the study surface had to be treated by spraying water on the earthen surface to create a wet sand layer up to about 5 cm thick, then a stone roller was used to grind the surface to make it level. Broken clay was evenly spread on the

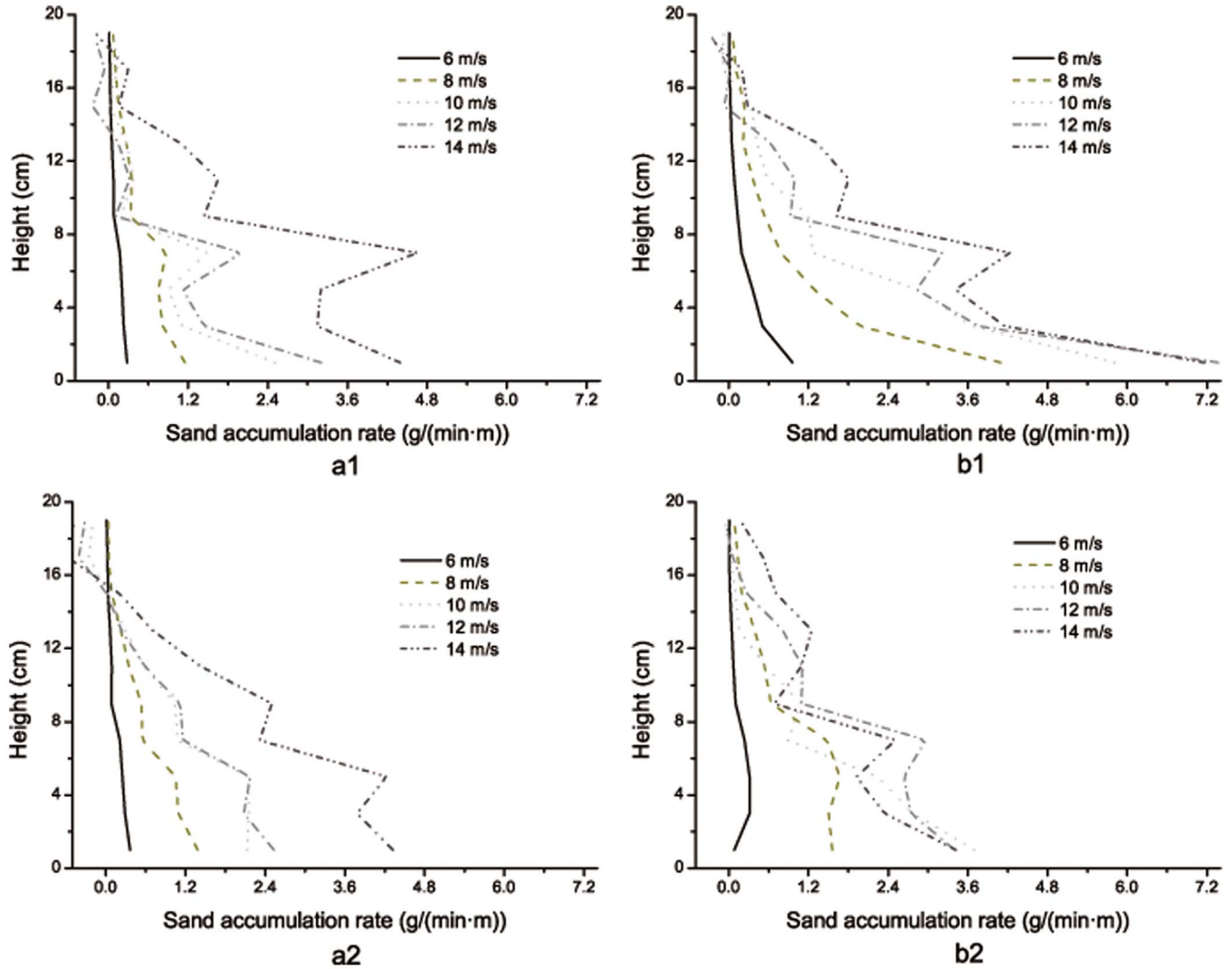

Figure 6 | Distribution of sand accumulation rates at various heights on the artificial gravel bed under different initial wind speeds. (a1) Variations in sand accumulation rates (g/(min·m)) at various heights on a medium gravel (2–4 cm) bed with coverage of 30% under different initial wind speeds (6 m/s, 8 m/s, 10 m/s, 12 m/s, and 14 m/s). (a2) On a medium gravel (2–4 cm) bed with coverage of 40%. (b1) On a large gravel (4–6 cm) bed with coverage of 30%. (b2) On a large gravel (4–6 cm) bed with coverage of 40%.

surface (each clay batch weighed about 0.5 kg/m^2) and a broom was used to mix the surface layer clay and the sand soil. The stone roller ground the surface level again. Then small gravel (diameter 0.5–2 cm) was evenly spread on the leveled earth surface, with a coverage of about 15%. The stone roller was used to compact the admixture again to increase earth surface hardness to an average measured value of $>$12 N/mm^2 as verified by a soil hardness tester. Then small gravel (diameter 1–2 cm) was once again evenly spread on the prepared earth surface, with a coverage of about 15%. Finally, gravels of different diameters were evenly spread on the treated earth surface at different coverage. For fair testing and equivalence, gravels of differing diameters were directly and randomly tossed onto non-treated surfaces.

Gravel paving to reduce aeolian sand transport and damage above the Mogao Grottoes began in 2009–2010. Our main study site was the typical original gravel bed topography and the artificial gravel bed formed after the installation of that paving. The original gravel bed topography was made up of cobbles, a mixed sand/gravel bed, and a sandy gravel bed. Gravel paving and sand covered 686,650 m^2, with coverage after ground treatment measured at 991,000 m^2, giving a total area of 1,677,650 m^2, approximately equivalent to the contiguous area of the original gravel bed. An area of shifting sands on nearby Mount Mingsha provided another small study block.

Wind tunnel experiments. Our gravel diameter sampling areas were set at 900 cm^2. We sampled from the four corners, the midpoints of the four sides, and the cross-point of two diagonals, producing a total of nine sampling spots. In each 900 cm^2 sampling plot, the diameters of 100 randomly selected gravels were measured and the average coverage in the original gravel bed calculated. Supplementary Fig. S3 online shows that the paved gravel on the original gravel bed was predominantly of small gravel ($\leq$2 cm). In 2004 the northern experimental area above the Mogao Grottoes had gravel coverage of 23.53% in its original gravel bed. Changes in sand coverage on gravel of different diameters, at different wind speeds and for different abrasion time, was studied based on field wind tunnel experimental data from 2004. Functional relations between gravel coverage, wind speed, and abrasion time were defined in 2004 field wind-tunnel experiments using small (average diameter 0.89 cm), medium (average diameter 2.68 cm) and large gravel (average diameter 5.49 cm).

The threshold wind speed (defined below) of aeolian sand above the grottoes was validated by field wind-tunnel (See Supplementary Fig. S4 online) experimental data extracted from the surface of a shifting sand area on Mount Mingsha in 2010. Wind speed outlines, sand transport, and sand accumulations in clean wind and sand-carrying wind conditions in gravel paving blocks with different gravel diameters and coverage were obtained from field wind-tunnel data collected in 2011.

Box-like sand-accumulation instruments (See Supplementary Fig. S5 online) of height 20 cm used in field wind tunnel experiments were set up at 3.4 m intervals on the gravel bed, spanning different gravel coverage and diameters. Weighed-out sand quantities (g) at different heights and the sand accumulation rates (g/(min·m)) on the gravel bed were calculated for different lengths of sand-carrying wind blowing times. A wind speed profiler with a pitot tube (See Supplementary Fig. S6 online) was also used.

Field experimental observations. Data pertaining to historical sand-accumulation conditions were obtained from sand-accumulation instruments with 16 orientations (Fig. 1) during 2004–2006. These reflected sand transport characteristics on the original gravel bed that had not been destroyed by paving. The transported sand, once collected, was weighed by electronic scales with +/−0.001 g precision.

During 2005–2008, data pertaining to wind speed and wind direction in the original gravel bed were obtained from the Japanese HOBO weather station (Fig. 1). By

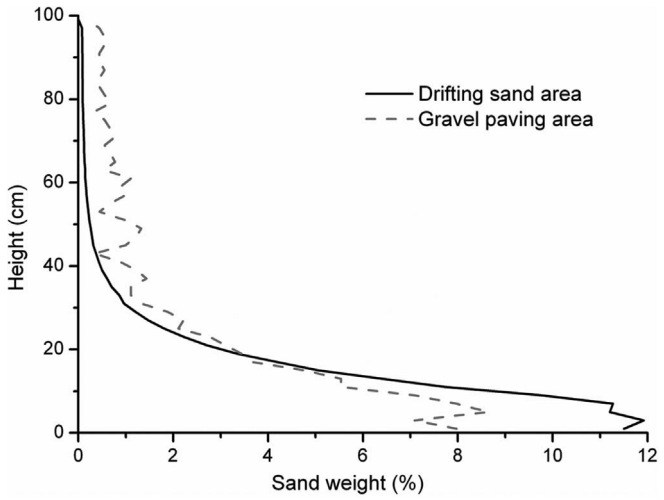

Figure 7 | Distribution of sand weights at various heights in the shifting sand area and the gravel paving area above the Mogao Grottoes during the great dust storm of June 2, 2011. The wind direction of the storm was northwest. Staged sand accumulation instruments of height 1 m were set up on the shifting sand area and the artificial gravel area along a NW → SE orientation.

combining field wind-tunnel experimental data and mathematical formulae, we extracted both wind speeds and wind directions.

This study reports the results from Area C in Fig. 1 (treated surface: large gravel, 30%; non-treated surface: medium gravel, 30%) and Area F (treated surface: medium gravel, 30%; non-treated surface: medium gravel, 30%). Wind speed and wind direction were extracted from automatic weather station data correlated with measured time intervals for sand weight in the sand-accumulation buckets. The local gravel bed sand-blowing and sand-carrying winds were assessed using data from the automatic weather station on above the grottoes for the dates March 18 – April 15, 2009 and May 13 – May 17, 2010. Sand weights collected by sand-accumulation buckets[21] in paved gravel experimental blocks with different treatments (dependent upon coverage, diameter, and construction technology) during these periods were used to study the impact and behavior, under natural conditions, of sand accumulation in paved gravel areas possessing various combinations of different gravel diameters and coverage. 11 sand-accumulation buckets were spaced 100 m apart on the northern side of a V-shaped nylon net (there were sand accumulation buckets in the original gravel bed and because buckets 10 and 11 were very close to the net and vulnerable to its effects, they were weeded out)[18]. The sand was weighed by electronic scales with +/−1 g precision.

The vertical heights of aeolian sand saltation and sand transport under natural conditions were measured using sand-accumulation instruments of height 1 m. These were set up on the surface of the shifting sand and artificial gravel bed areas along a NW → SE orientation above the grottoes during a large dust storm (northwest wind) on June 2, 2011. These staged sand-accumulation instruments (with openings at 2 cm increments) measured the intensity of the dust storm; electronic scales with +/−0.01 g precision were used to measure sand weights from different heights.

1. Wu, Z. *Geomorphology of wind-drift sands and their controlled engineering.* Wu, Z. (ed.), 31–42 (Science Press, Beijing, 2003).
2. Li, G. S. *et al.* Study on temperature and humidity environment of grotto 72 at the Mogao Grottoes in Dunhuang, China. *Int. J. Climatol.* **33**,1863–1872 (2013).
3. Li, G. S., Qu, J. J., Wang, W. F. & Yang, W. Overall efficiency of a V-shaped nylon net fence in preventing sand damage to the Mogao Grottoes. *Sci. Cold Arid Reg.* **4**, 0163–0174 (2012).
4. Redway, J. W. The dust of the *Gobi*. *Ecology* **2**, 21–25 (1921).
5. Osborn, H. F. Methods and results of the American Museum expeditions in the Gobi Desert, 1922–25. *Nature* **118**, 198–199 (1926).
6. Parungo, F., Li, Z., Li, X., Yang, D. & Harris, J. Gobi dust storms and the Great Green Wall. *Geophys. Res. Lett.* **21**, 999–1002 (1994).
7. Jugder, D. *et al.* Spatial and temporal variations of dust concentrations in the Gobi Desert of Mongolia. *Global Planet. Change* **78**, 14–22 (2011).
8. Zhou, D. G. & Huang, R. H. Characterization of turbulent flux transfer over a Gobi surface with quality-controlled observations. *Sci. China Earth Sci.* **54**, 753–763 (2011).
9. Nickling, W. G. & Neuman, C. M. Development of deflation lag surfaces. *Sedimentology* **42**, 403–414 (1995).
10. Dong, Z. B., Qu, J. J., Liu, X. P., Zhang, W. M. & Wang, X. M. Experimental investigation of drag coefficients of gobi surfaces. *Sci. China Earth Sci.* **45**, 609–615 (2002).
11. Mikami, M. *et al.* Measurement of saltation process over gobi and sand dunes in the Taklimakan Desert, China, with newly developed sand particle counter. *J. Geophys. Res. Atmos.* **110**, D18S02 (2005).
12. Zhang, K. C., Qu, J. J., Zu, R. P. & Ta, W. Q. Characteristics of wind-blown sand on *Gobi*/mobile sand surface. *Environ. Geol.* **54**, 411–416 (2008).
13. Gao, Z. Q. *et al.* Study of roughness lengths and drag coefficients over Nansha Sea region, *Gobi*, desert, oasis and Tibetan plateau. *Phys. Chem. Earth Part B: Hydrol. Oceans Atmos.* **25**, 141–145 (2000).
14. Bagnold, R. A. The effect of sand movement on the surface wind. *The physics of blown sand and desert dunes.* Bagnold, R. A. (ed.), 57–76 (Springer, Netherlands, 1971).
15. Lettau, K. & Lettau, H. Experimental and micrometeorological field studies of dune migration. *Exploring the world's driest climate.* Lettau, H. H. & Lettau, K. (ed.), 110–147 (Madison, Wisconsin, 1978).
16. Qu, J. J., Huang, N., Dong, G. R. & Zhang, W. M. The role and significance of the Gobi Desert pavement in controlling sand movement on the cliff top near the Dunhuang Mogao Grottoes. *J. Arid Environ.* **48**, 357–371 (2001).
17. Dong, Z. B., Liu, X. P. & Wang, X. M. Aerodynamic roughness of gravel surfaces. *Geomorphology* **43**, 17–31 (2002).
18. Liu, B. L., Zhang, W. M., Qu, J. J., Zhang, K. C. & Han, Q. J. Controlling windblown sand problems by an artificial gravel surface: A case study over the gobi surface of the Mogao Grottoes. *Geomorphology* **134**, 461–469 (2011).
19. Tan, L. H., Zhang, W. M., Liu, B. L., An, Z. S. & Li, J. G. Simulation of wind velocity reduction effect of gravel beds in a mobile wind tunnel atop the Mogao Grottoes of Dunhuang, China. *Eng. Geol.* **159**, 67–75 (2013).
20. Zhang, W. M., Wang, T., Wang, W. F. & Liu, B. L. Wind tunnel experiments on vertical distribution of wind-blown sand flux and change of the quantity of sand erosion and deposition above gravel beds under different sand supplies. *Environ Earth Sci* **64**, 1031–1038 (2011).
21. Zhang, W. M. *et al.* Variation of gobi sand transport amout under multi-wind directions. *J. Desert Res.* **31**, 543–549 (2011).

Acknowledgments

This research was partially supported by the National Science and Technology Support Program (2013BAC07B02, 2012BAC08B07), the National Natural Science Foundation of China Key Program (40930741), the National Science Foundation of China (41001005) and Civil Test Application Data Processing (Y1141401SN). Sincerely thanks Wei Min Zhang for providing part of the data and Liang Ying Sun for many suggestions, especially thanks Edward Derbyshire for many constructive comments. We are grateful to Wei Min Zhang, Li Hai Tan, Ke Cun Zhang, Zhi Shan An, Ben Li Liu, Guo Bin Zhang, Fei Qiu, Hong Tao Zhan, Xiang Ru Lin and Rui Li for their assistance with experiments.

Author contributions

G.S.L., J.J.Q. and X.Z.L. wrote the manuscript text, J.J.Q. and W.F.W. offered fund and designed part of the study. All authors discussed the results and contributed to the manuscript.

Additional information

Supplementary information accompanies this paper at http://www.nature.com/scientificreports

Competing financial interests: The authors declare no competing financial interests.

How to cite this article: Li, G.S., Qu, J.J., Li, X.Z. & Wang, W.F. The sand-deposition impact of artificial gravel beds on the protection of the Mogao Grottoes. *Sci. Rep.* **4**, 4341; DOI:10.1038/srep04341 (2014).

This work is licensed under a Creative Commons Attribution-NonCommercial-NoDerivs 3.0 Unported license. To view a copy of this license, visit http://creativecommons.org/licenses/by-nc-nd/3.0